Theoretical Studies on the Mode of Inhibition of Ribonucleotide Reductase by 2′-Substituted Substrate Analogues

Pedro Alexandrino Fernandes and Maria João Ramos*[a]

Abstract: Several 2′-substituted-2′-deoxyribonucleotides are potent time-dependent inactivators of the enzyme ribonucleotide reductase (RNR), which function by destructing its essential tyrosil radical and/or by performing covalent addition to the enzyme. The former leads to inhibition of the R2 dimer of RNR and the latter to inhibition of the R1 dimer. Efforts to elucidate the mechanism of inhibition have been undertaken in the last decades, and a general mechanistic scheme has emerged. Accordingly, two alternative pathways lead either to the inhibition of R1 or R2, for which the 2′-chloro-2′-deoxynucleotides serve as the model for the inhibition of R1 and the 2′-azido-2′-deoxynucleotides the model for the inhibition of R2. However, the underlying reason for the different behavior of the inhibitors has remained unknown until now. Moreover, a fundamental mechanistic alternative has been proposed, based on results from biomimetic reactions, in which the 2′-substituents would be eliminated as radicals, and not as anions, as previously assumed. This would lead to further reactions not predicted by the existing mechanistic scheme. To gain a better understanding we have performed high-level theoretical calculations on the active site of RNR. Results from this work support the general Stubbe's paradigm, although some changes to that mechanism are necessary. In addition, a rational explanation of the factors that determine which of the dimers (R1 or R2) will be inactivated is provided for the first time. It has been demonstrated also that the 2′-substituents are indeed eliminated as anions, and not as radicals. Biomimetic experiments have led to different results because they lack a basic group capable of deprotonating the 3′-HO group of the substrate. It has been found here that the chemical character of the leaving group (radical or anionic) can be manipulated by controlling the protonation state of the 3′-HO group.

Keywords: density functional calculations · enzymes · inhibitors · ribonucleotide reductases

Introduction

Ribonucleotide reductases (RNRs) are fundamental enzymes present in all living organisms. They catalyze the reduction of ribonucleotides to 2′-deoxyribonucleotides, the rate-limiting step in DNA replication and repair.[1–6] They play a prominent role in the regulation and control of cell replication, and have recently emerged as a promising target for the design of new chemotherapeutics for antitumor and antiviral treatments.[5,7–10] The inactivation of the enzyme results in significant antiproliferative effects against a wide range of tumor cell lines,[10–12] as well as human xenografts in mice.[10,13,14] Recently, Gemcitabine 5′-diphosphate (2′,2′-difluoro-2′-deoxycitidine-5′-diphosphate) has been approved for the treatment of non-small cell lung cancer in Europe and pancreatic cancer in the United States.[15,16] RNRs are divided in three classes according to the cofactors required for catalytic activity. Evidence that all of them follow a radical mechanism to dehydrate the substrate has been obtained in the last decades. Class I RNRs possess a stable tyrosyl radical adjacent to a diiron cluster.[17,18] Class II RNRs use AdoCbl as cofactor.[19,20] Class III RNRs are expressed in an anaerobic environment and possess a glycyl radical generated by a FeS cluster.[21,22] This study is devoted to class I RNRs. The *E. coli* RNR has been extensively investigated and is considered as a prototype for the mammalian protein.[2–4] It is a $\alpha_2\beta_2$ tetramer, constituted by two homodimers. The dimers must associate to catalyze nucleotide reduction. When separated, none of the dimers presents any catalytic activity.[4] The α_2 dimer (R1 subunit) has a molecular weight of 171 kDa; the β_2 dimer (R2 subunit) has a molecular weight of 87 kDa and (in Class I RNR) it possesses a

[a] Prof. M. J. Ramos, P. A. Fernandes
REQUIMTE/Faculdade de Ciências do Porto
Rua do Campo Alegre, 687
4169007 Porto (Portugal)
Fax: (+351) 22-6082959
E-mail: mjramos@fc.up.pt

Supporting information for this article is available on the WWW under http://www.chemeurj.org or from the author: Molecular coordinates for all stationary points.

DOI: 10.1002/chem.200304948

stable tyrosil radical adjacent to a diiron cluster.[17,18] The tyrosil radical is generated in the R2 subunit, presumably through hydrogen abstraction by the oxo-bridged diiron center, located ~30 Å away from the active site. The radical is transferred from Tyr122 in R2 to C439 at the active site in R1. Although the detailed transfer mechanism is unknown, it is believed that the transfer occurs through a conserved chain of hydrogen-bonded residues.[26] The X-ray crystallographic structure of this enzyme with the bound substrate has been determined, and the portion corresponding to the active site is shown in Figure 1.[27] Five conserved residues,

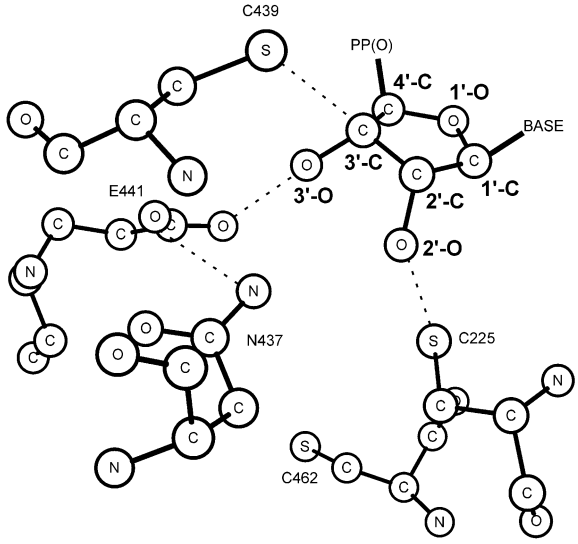

Figure 1. X-ray structure of the active site of ribonucleotide reductase with the bound substrate. Relevant atom numbering is presented in the inhibitor.

namely three cysteines (C225, C439, and C462), one glutamate (E441), and one asparagine (N437) have been established as necessary for catalysis.[28,29]

In 1976 Thelander and Larsson discovered that 2-chloro-2′-nucleosides-5′-diphosphates (N*cl*DP) and 2′-azido-2′-nucleosides-5′-diphosphates (N*z*DP) were potent inactivators of RNR, although they act in very different ways. N*cl*DP inhibits R1 without affecting R2, by covalent addition of a reaction intermediate to the enzyme. N*z*DP inhibits R2 without affecting R1, by destroying the essential tyrosyl radical of R2.[30] Stubbe and Kozarich found later that 2′-fluoro-2′-nucleosides-5′-diphosphates (N*f*DP) behave similarly to N*cl*DP.[31] Since then, the inactivation mechanism by 2-substituted nucleotides has been extensively studied,[10,32–55] and a general pattern has emerged (Scheme 1).

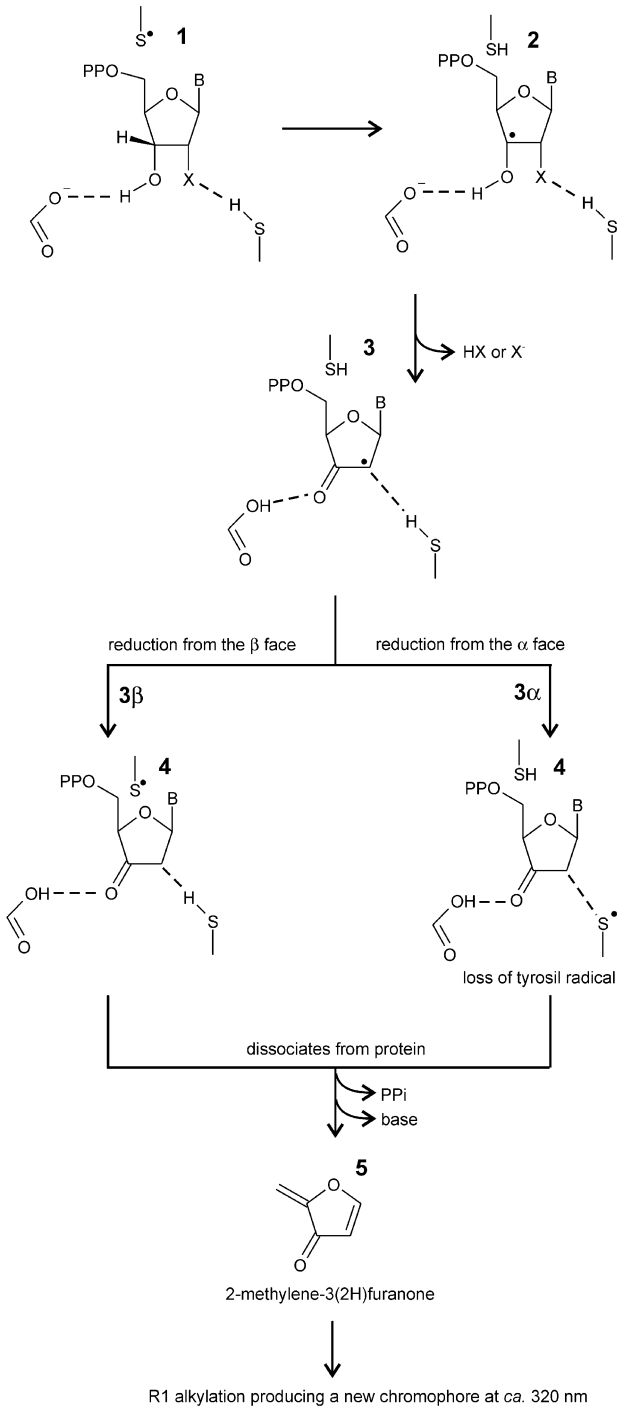

Scheme 1. The general paradigm for RNR inhibition by 2′-substituted substrate analogues, according to reference [45].

The reaction begins by abstraction of the 3′-H of inhibitor **1** by radical C439 to give the 3′ radical **2**. This first step is similar to the mechanism of the natural substrate. In a second step, X is eliminated as X^- (or HX) and a proton is transferred from the 3′-HO group to E441, resulting in the 2′-ketyl radical **3**. This radical abstracts a hydrogen atom either from C225 in the α-face (**3**α), or from C439 in the β-face (**3**β), both resulting in the stable closed-shell ketone **4**. In the latter case the radical is regenerated in R2, and inhibition results from covalent addition of the furanone derivative **5** (2-methylene-3(2*H*)-furanone) to R1, most probably to a lysine residue. The furanone is formed in solution upon dissociation and subsequent chemical decomposition of the ketone **4**. Nucleophiles such as dithiothreitol, when present in solution, protect the enzyme against alkylation by **5**. In the former case, inhibition results from destruction of the essential tyrosil radical in R2. The furanone **5** is generated in solution as well, and subsequently it also inactivates R1.

N*cl*DP became the model for the first type of inactivation and N*z*DP became the model for the second type of inactivation. However, the reason why they behave differently has remained unknown.

Recently, a new fundamental alternative to the mechanism presented in Scheme 1 was proposed. It is based on compelling results from biomimetic reactions, where it was unambiguously demonstrated that 2′-chloro-2′-deoxy-5′-*O*-(*tert*-butyldimethylsilyl) nucleosides and 2′-chloro-2′-deoxy-3′-phenoxythiocarbonil-5′-*O*-(*tert*-butyldimethylsilyl) nucleosides, upon selective generation of 3′radicals in refluxing toluene, eliminated radical chlorine, instead of chloride. The latter nucleosides displayed the same behavior with azide (instead of chlorine) in the 2′position, although in the former the azide was reduced to amine.[46] The substrate analogue 2′-chloro-2′-deoxy-6′-*O*-nitrohomouridine also eliminated radical chlorine under similar conditions, to give 2-(2-hydroxyethyl)-3(2*H*)-furanone, an analogue of **5.**[47–49] That would imply that the 2′-substituents, eliminated as radicals, would need to react further with (probably) the active site cysteines, to regenerate the radical at the active site, and dissociate into solution as anions, which are the detected products of the enzymatic reaction.

Based on these results, and considering earlier mechanistic results with other 2′-substituted nucleotide analogues, we have explored the mechanism of these important reactions, to try to shed some light on to the chemical nature of the eliminated 2′-substituents, and to understand the factors that determine which of the dimers (R1 or R2) will be inactivated by each inhibitor.

Methods

Density functional theory was used in all calculations, with the Gaussian98 suite of programs,[57] at the unrestricted Becke3LYP level of theory.[58–60] The 6-31G(d) basis set was used for geometry optimizations, and to calculate the zero-point, thermal and entropic contributions. It is well known that larger basis sets give very small additional corrections to the above mentioned properties, and their use is hence considered unnecessary from a computational view.[61–63] The much larger 6-311+G(2d,2p) basis set was used to calculate the final electronic energies. This basis set is close to saturation in the present system. The calculations were performed as follows: first, the transition states for each mechanistic step were located and optimized. Internal reaction coordinate calculations, followed by further tighter optimizations, were performed to confirm which minima were connected to each transition state. A frequency analysis was performed at each stationary point on the potential energy surface. All stationary points were characterized by the number of imaginary frequencies (none for minima and only one for transition states). A scaling factor of 0.9804 was used for the vibrational energies. Thermal and entropic effects were calculated at physiological temperature. According to previous studies on active sites in proteins, the introduction of a dielectric continuum in the calculations with an empirical dielectric constant of 4 gives good agreement with experimental results, and accounts for the average effect of both the protein and the buried water molecules.[26,61,63,64] As our system contains charged species, it is important to evaluate the influence of the environment on the energetics. Coherently, all energies were calculated under the influence of a dielectric continuum. To this purpose we have used a Polarized Continuum Model, named C-PCM, as implemented in Gaussian98.[57] This method considers the solute as a set of interlocking spheres, centered in each atom, with apparent surface charges, that interact with the wave function. The continuum is modeled as a conductor, instead of a dielectric. This simplifies the electrostatic computations, and corrections are made *a posteriori* for dielectric behavior. The contribution of the continuum was calculated with the larger 6-311+G(2d,2p) basis set. Enzymes have highly anisotropic charge distributions, which give them the capacity to achieve specific stabilizing effects. Those specific electrostatic effects are included in the models through the explicit inclusion of the corresponding amino acids. The continuum thus represents the long-range interaction of the active site with the isotropic remaining part of the enzyme.

The hydrogen-bonded complexes illustrated in this work have a very large number of minima. The particular structures discussed here were the ones that most closely reproduced the geometry of the active site. So, they are not necessarily the absolute minima for the complexes.

In open-shell systems, spin contamination is a frequent problem. It is well known that DFT methods are quite robust to spin contamination, and in the calculations presented here, the expectation value for S^2 never reached a value of 0.78, before annihilation. After annihilation, the expectation value for S^2 never exceeded 0.7501. Atomic charges and spin density distributions were calculated with a Mulliken population analysis,[65] using the larger basis sets.In the calculations we have used the following models for the residues of the active site: the cysteines were modeled by methylthiol molecules, the glutamate by a formate, the asparagine by methylamide, and the substrate analogues were modeled without the base and the diphosphate. The adequacy of these models was demonstrated in earlier works.[61,63,66] The geometry of the resulting active site model is very similar to the enzyme active site, as can be seen by comparing Figure 1 (X-ray) with Figure 2 (models). We must keep in mind that the X-ray structure in Figure 1 includes the natural substrate, whereas the models include N*cl*DP and N*z*DP. Another difference is that C439 in the X-ray structure is protonated and in the models is in the radical form (and is already attacking H3′ in Figure 2). So, we are not comparing structures that should be expected to be superimposable.

The topography of the active site is retained in the models, with all gas phase residues in their correct position, and retaining the important network of hydrogen bonds seen in the X-ray structure (E441 to O3′ and to N437, and C225 to the 2′ position (Cl or N_3). The most noticeable difference is in the orientation of the oxygen of N437 and the methyl group of C225. Upon optimization in gas phase these two groups turned one to each other to make hydrogen bonds. This has a very small effect in the reactions studied, and in general we can say that the gas phase models reproduce very well the active site geometry.

Results and Discussion

Decomposition of the inhibitors: The first mechanistic step in the normal catalytic pathway corresponds to the abstraction of the 3′-H atom by the radical C439. This step is uncontroversial, as it is well supported by experimental evidence.[51] It was thus assumed in Scheme 1 that the first step of the decomposition of the inhibitor would be similar to the normal catalytic pathway. We started by investigating such a step; however, the results were different than expected. We found that for both inhibitors, the hydrogen atom abstraction, the subsequent proton transfer from the 3′-HO to E441, and the elimination of the 2′-substituent were fully coupled, and occurred in a single mechanistic step, through a single transition state. Therefore, substrate **1** decomposes spontaneously and directly to the open-shell 2′-ketyl radical **3** upon activation. The 3′radical **2** in Scheme 1 is not a stationary point on the potential energy surface.

Interestingly, the inhibition mechanism has already deviated from the normal pathway, since the natural substrates do not eliminate spontaneously the 2′-HO group. Elimination of the 2′-HO must be assisted by protonation.[63] The

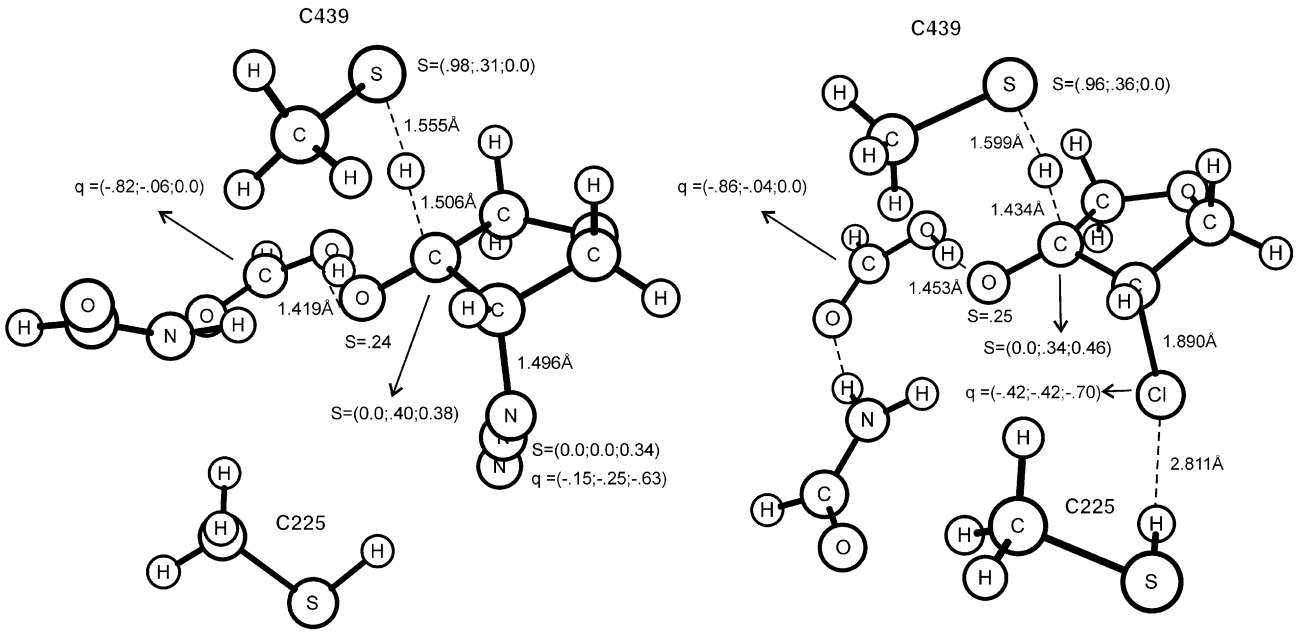

Figure 2. Transition states for the abstraction of the 3′-H atom of N*z*DP (left) and N*cl*DP (right) by C439. All distances in Ångström and spin densities in a.u.

transition states associated with this step are shown in Figure 2 for both inhibitors.

The transition states are very similar. Considering N*cl*DP, the transition state is achieved with the hydrogen atom shared between the inhibitor and the sulfur atom of C439. At this point the proton of the 3′-HO group is already transferred to E441, and hydrogen-bonded to 3′-O. In the reactants the proton was bound to 3′-O, and hydrogen-bonded (1.640 Å) to E441. The 2′-C–Cl bond is slightly elongated, from 1.833 Å in the reactants to 1.890 Å in the transition state; this already reflects the tendency of the substituent to be eliminated. The conserved hydrogen bond between C225 and the 2′-substituent shortens when going from the reactants (2.878 Å) to the transition state (2.811 Å), due to the increasing charge of the chloride. In the products the 3′-H is transferred to the thiol group of C439, and the 2′-substituent is fully eliminated as a chloride ion. It becomes strongly hydrogen-bonded to the thiol group of C225, with an even shorter bond length of 2.503 Å.

Concerning the spin density, it mainly moves from the sulfur atom of C439 to the 2′-C atom. The spin density delocalizes also to the 3′-O atom (0.21 a.u. in the products) due to the keto–enol equilibrium, and to the chloride ion, which still retains a small radical character (0.18 a.u.). Analysis of the charge distribution in the reactants and the products shows that during the reaction the charge moves from E441 to the chloride. This last result has very important implications, since it clearly shows that the 2′ substituent is eliminated as anionic chloride, and not as radical chlorine, contrary to the mechanism previously proposed and unambiguously demonstrated with biomimetic reactions.[46–49] The reason for this discrepancy was explored in this work, and will be explained later (see Biomimetic Experiments).

The transition state obtained for the first step with the inhibitor N*z*DP is similar to the one previously described. The 3′-H atom is also shared between the inhibitor and the sulfur atom of C439. The proton of the 3′-HO group has been also already transferred to E441, and hydrogen-bonded to 3′-O. In the reactants the proton was bound to 3′-O, and hydrogen-bonded (1.591 Å) to E441. The 2′-C–N bond is slightly elongated, from 1.478 Å in the reactants to 1.496 Å in the transition state. This effect is less pronounced with N*z*DP than with N*cl*DP. In the products the 3′-H atom is transferred to the thiol group of C439, and the azide group is eliminated from the ring and becomes located below the α face of N*z*DP, under the 2′-C–3′-C bond. The spin density shifts from the sulfur atom of C439 to the 2′-C atom. The spin density delocalizes also to 3′-O atom (0.17 a.u. in the products) due to the keto-enol equilibrium, and most significantly to the azide group, after it eliminates from the inhibitor.

Analysis of the charge distribution in the reactants and the products shows that during the reaction the charge delocalizes from E441 to both the inhibitor and the azide. In the products the protonated glutamate is neutral, the inhibitor retains a total charge of −0.27 a.u. and the azide has a total charge of −0.63 a.u. This result strongly suggests that the azide is also eliminated as an anion, like in the previous case, although the spin density is still shared with the azide in the complex of the products.

The energetics of the two previous reactions is also similar. The activation free energy for N*z*DP corresponds to 7.0 kcal mol^{-1} and for N*cl*DP it amounts to 5.7 kcal mol^{-1}. In one of our previous studies using the natural substrate,[37] an activation enthalpy of 7.2 kcal mol^{-1} was obtained with a similar model (without C225) and theoretical level, com-

pared to the 5.6 kcal mol^{-1} and 3.4 kcal mol^{-1} enthalpy barriers for N*z*DP and N*cl*DP obtained here. We can thus conclude that activation of the inhibitors occurs faster than the natural substrate, although the difference is small. The reaction with both inhibitors is exothermic, having a reaction free energy of -7.9 kcal mol^{-1} and -19.5 kcal mol^{-1} for N*z*DP and N*cl*DP, respectively. The reaction free energy is lower with N*cl*DP due to the strong hydrogen bonds between the chloride ion and C225 (and also N437) present in the products.

Reduction of the 2′-C radical: We initially analyzed the reduction of the 2′-C radical generated in the previous steps. Each inhibitor was studied separately, beginning with N*cl*DP. At this point the system has two redox-active cysteine groups, C225 and C439, both capable of transferring a hydrogen atom to 2′-C, leading to the well-established intermediate ketone **4**. Inspection of the products of the last mechanistic step reveals that the two cysteine groups are not in equivalent steric and energetic conditions to transfer the hydrogen atom. At the beginning of the catalytic cycle, C225 was better positioned to reduce a radical at the 2′ position. It was hydrogen-bonded to the chlorine atom at 2′-C, in agreement with the X-ray structure of the active site of RNR with the natural substrate, where it is hydrogen-bonded to the 2′-HO group, and is known to transfer a proton to the 2′O atom in the normal catalytic pathway.[1,61] C439 is not so well positioned to reduce the 2′ position, as it ponits directly at 3′-C and is known to react invariably with the 3′-H atom in the first step. However, after the elimination of chloride, the hydrogen atom of the thiol group of C225 becomes strongly hydrogen-bonded to the chloride. This newly formed hydrogen bond hinders the access of the thiol group of C225 to 2′-C, as it must decomplex the anion prior to reaction with 2′-C. The other cysteine (C439) group does not face such hindrance to access the 2′-C radical. We have studied the reduction of the radical with each cysteine in turn, beginning with C439.

Figure 3 shows the transition state for the hydrogen atom transfer from C439 to 2′-C. The transition state is similar to the one found for the first step. The hydrogen atom is shared between the 2′-ketyl radical and the sulfur atom of C439. In the reactants both the 3′-C–3′-O and the 2′-C–3′-C bond lengths lie between those for typical single and double bonds, due to the delocalization of the radical between 2′-C and 3′-O (1.255 Å and 1.413 Å, respectively). C225 becomes strongly hydrogen-bonded to the chloride ion. In the products the thiol hydrogen atom is transferred to the 2′-C atom, which makes the 2′-C–3′–C a typical single bond (bond length: 1.516 Å) and the 3′-C–3′-O a typical double bond (bond length: 1.222 Å). The distance between the chloride ion and 2′-C increases upon reduction, from 2.678 Å to 3.402 Å, as predictable. However, the hydrogen bonding pattern between chloride and the residues C255 and N437 in the active site remains almost unchanged.

During the reaction the spin density shifts to the sulfur atom of C439. Coherently, the spin densities at 2′-C, 3′-O, and Cl^- are zero in the products. The charge is even more localized at the chloride in the products (-0.73 a.u.). The activation free energy for this reaction corresponds to 12.6 kcal mol^{-1}. The reaction is almost thermoneutral, with a reaction free energy of 0.4 kcal mol^{-1}.

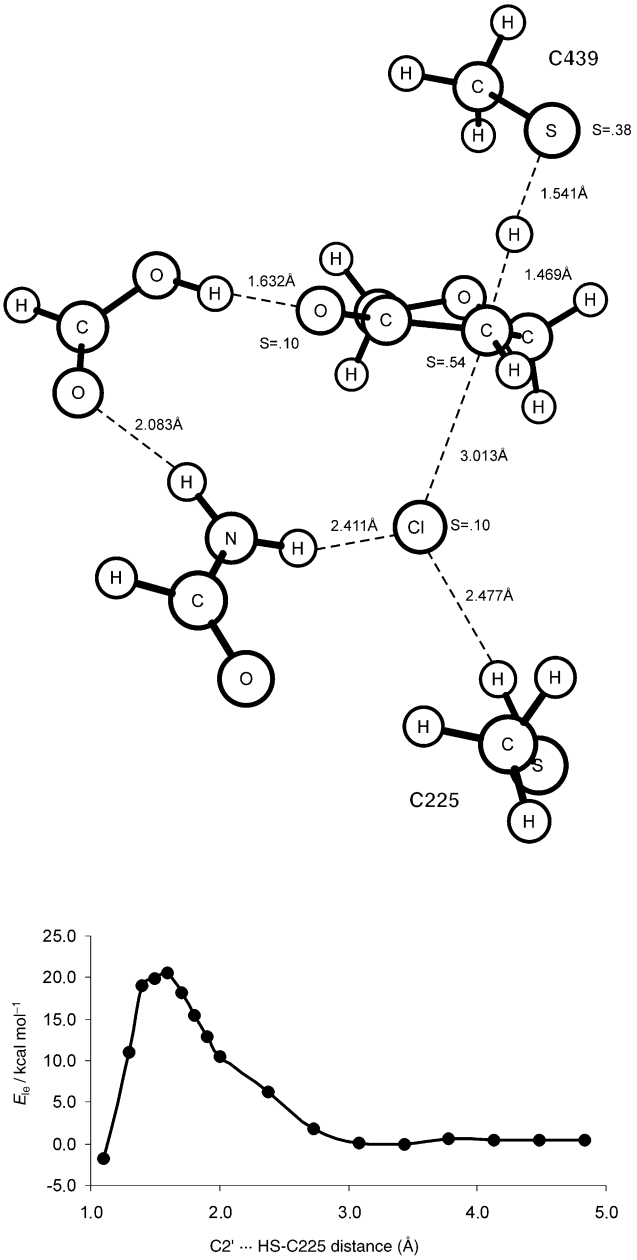

Figure 3. Top: Transition state for reduction of the 2′-C radical by C439. All distances in Å and spin densities in a.u. Bottom: Relaxed potential energy surface scan along the 2′-C-HS-C225 coordinate.

We then studied the other alternative, that is reduction of the 2′-C radical by C225. We started by performing a relaxed potential energy surface scan along the 2′-C–thiol distance, to be able to make an educated guess at the transition state. The results from the scan are depicted in Figure 3 (bottom). During the scan we confirmed that C225 was hindered to approach the 2′-C atom by the chloride ion, and that it decomplexes the ion before approaching the transition state. Breaking (even partially) such a hydrogen bond

has a high energetic cost, and from the scan we were able to estimate the barrier to be about 21 kcal mol^{-1}. At this point we saw no reason to refine further the transition state and the reactants, since such refinement would lower the energy of the minimum and increase the energy of the transition state, thus increasing even further the barrier, which was already very high compared to that for the alternative reaction with C439.

From these results we can understand, for the first time, why N*cl*DP inhibits R1 without affecting R2. The main reason is that the 2′ substituent is eliminated as an anion, which becomes strongly hydrogen-bonded to C225, which in turn hinders its access to 2′-C. This makes reduction by C439 faster, and hence allows the regeneration of the radical in C439, and consequently, in R2. It seems that in general 2′ substituents that become hydrogen-bonded to C225 will inhibit R1 without affecting R2. Another example of this concerns the 2′-fluoro-2′-deoxynucleotides, which are shown to behave like their chloro analogues, inhibiting R1 without affecting R2.[31] It seems obvious now that in this case the substituent will also be eliminated as an anion and will trap the thiol of C225, forcing reduction by C439.

In previous work,[56] which focused on the full mechanism of inhibition of RNR by N*z*DP, it was found that the next step upon activation in the most favorable pathway is addition of azide to C3′. The azide is already in a good position to attack the C3′ atom, and the reaction proceeds with a free energy barrier of 16.6 kcal mol^{-1}.[56] The addition of the azide to C3′ is consistent with conclusions from several other experimental studies,[1,43,67] and so we did not repeat the calculation for that step because the result would be equivalent to the one from reference [56]. Thus we continued from the next intermediate, that is a structure in which the azide is bound to the 3′-C atom. The obvious consequence of this is that C225 is not hindered anymore from reaching the 2′-C atom, and now both cysteine groups are in a good position to reduce the 2′-ketyl radical. We have studied each reaction in turn and the corresponding transition states are given in Figure 4.

Concerning the hydrogen atom transfer from C225, at the transition state the hydrogen atom is located between the inhibitor and the thiol sulfur atom. Contrary to the other similar transition states shown above, the hydrogen atom is closer to the sulfur atom than to the inhibitor. This means that this is an early transition state, whose geometry is close to that of the reactants, and hence should have a lower barrier than the previous ones. In the reactants the thiol bond is 1.356 Å long and the distance from the thiol hydrogen atom to the 2′-C atom is 3.501 Å. In the products the hydrogen atom is bound to the 2′-C atom and the cysteine group moves to 4.360 Å from the transferred hydrogen atom.

The spin density shifts from the 2′-C atom to the sulfur atom of C225. Notably, the spin pattern only changes slightly until the transition state is achieved, and more extensive changes occur only after the transition state. The activation

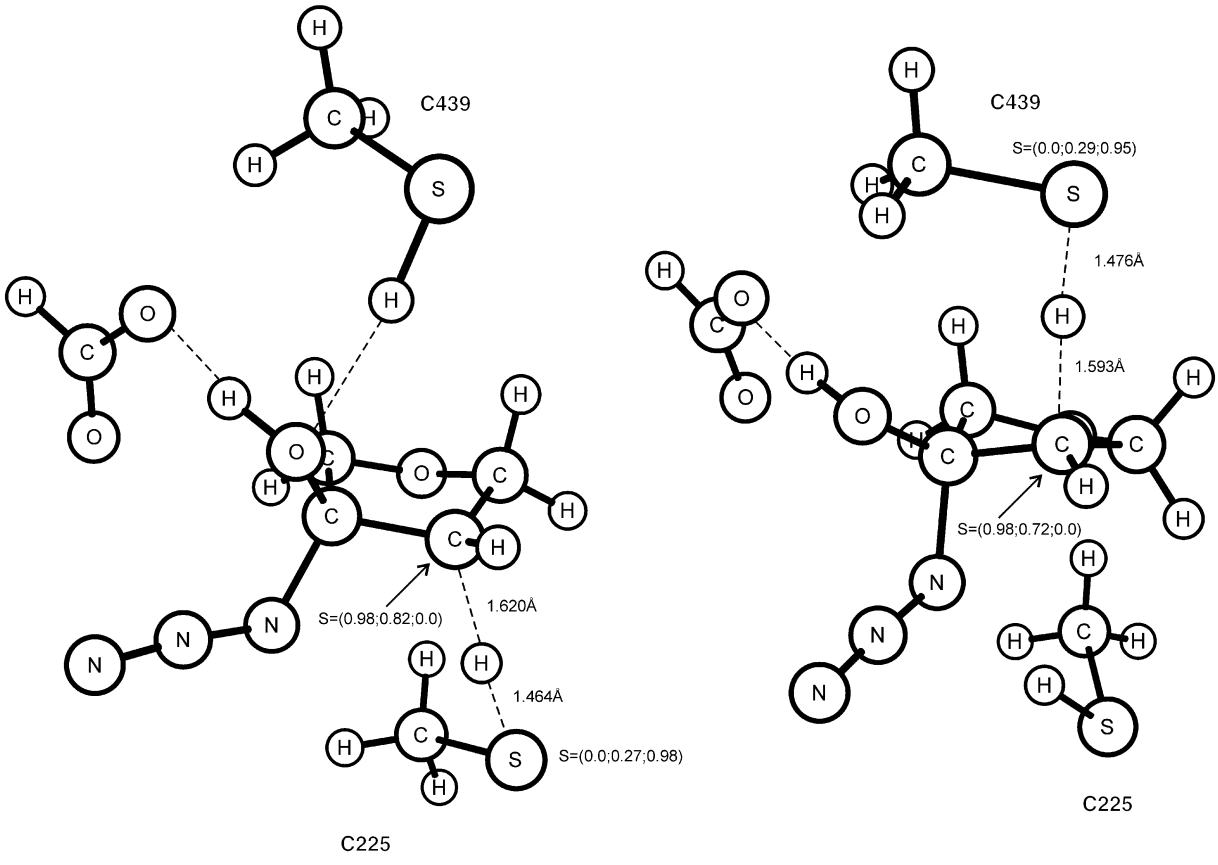

Figure 4. Transition state for reduction of the 2′-C radical by C225 (left) and C439 (right). All distances in Å and spin densities in a.u.

free energy for this reaction is lower than that for the previous reactions, consistent with an earlier transition state, corresponding to only 9.0 kcal mol^{-1}. The reaction is exothermic, with a reaction free energy of -8.3 kcal mol^{-1}.

Reduction can also be carried out by C439. The transition state for this reaction is depicted also in Figure 4 (right). The hydrogen atom lies between the inhibitor and the thiol sulfur atom of C439. The hydrogen atom is also closer to the sulfur atom than to the inhibitor, which reveals another early transition state, probably with a low barrier too. In the reactants the thiol bond is 1.356 Å long and the distance from the thiol hydrogen atom to the 2′-C atom is 3.349 Å. In the products the hydrogen adds to the 2′-C atom and the cysteine group moves to its former position, close to the 3′-C position and hydrogen-bonded to E441. The spin density shifts from the 2′-C atom to the sulfur atom of C439. The spin pattern again changes only slightly until the transition state is reached, and then more extensively after it. The activation free energy for this exothermic reaction is very slightly lower than that for the previous reaction (7.9 kcal mol^{-1}), with a reaction free energy of -10.1 kcal mol^{-1}.

If we consider only the free energy barriers, we can say that the hydrogen atom transfer is kinetically equivalent from both cysteine groups in the active site. Indeed, the difference between them (1.1 kcal mol^{-1}) is too small to be meaningful, and the high-level theoretical method used has an uncertainty of about 2.5 kcal mol^{-1}. The transition state geometries and the spin density distributions are also almost equivalent for both reactions. However, transfer from each cysteine group has a very different consequence for the enzyme; transfer from C225 will destroy the tyrosyl radical and inhibit R2, whereas transfer from C439 will regenerate the tyrosyl radical, and inhibit R1. Experimental data confirm that the second is the one that happens with N*z*DP, but does not explain the reason for it.

High level theoretical calculations can determine the barriers associated with the chemical steps, which usually dominate the mechanisms. In this case we have demonstrated that both reactions are chemically equivalent, and therefore the steric factors become dominant. These can not be obtained quantitatively by the present models, but here their relative magnitude can be determined unambiguously. Hence, we can see in the X-ray structure that C225 is already hydrogen-bonded to the 2′-C position, and there are several pieces of evidence that it reacts with the 2′-C atom in the normal catalytic pathway. Thus, no significant conformational change is needed for the reaction to proceed. Inversely, C439 is not hydrogen-bonded to 2′-C but instead to 3′-HO, which has moved to the β face upon addition of the azide to 3′-C. Similarly, in the X-ray structure, C439 is interacting with the 3′-H atom, which was originally in the β face; moreover, it has been demonstrated experimentally that the initial C439 radical always reacts with the hydrogen in the 3′ position, and never with the hydrogen atom in the 2′ position. As both hydrogen atoms are chemically equivalent, the ability of C439 to react with the 3′-H atom only results from the hindrance of C439 reaching the 2′-H atom first, which means that conformational energy would be needed to achieve it. As a result, this reaction becomes dominated by steric factors, and not by the chemical step. In the present case, the steric rearrangement of the active site unambiguously favors hydrogen transfers from C225 to the 2′-C atom. This factor is dominant because the chemical steps are equivalent, a situation similar to that in the first mechanistic step. Thus we can conclude that the reason why N*z*DP inhibits R2 is the favored steric position of C225 over C439 to reduce 2′-C, since both steps are chemically equivalent.

Biomimetic experiments: During the last decade, a set of biomimetic experiments were performed, to reproduce several aspects of the mechanism of ribonucleotide reductase. Those experiments proved to be very useful in several aspects. Giese and co-workers studied the dehydration of an analogue of the natural substrate, showing that elimination of the 2′-HO group is subject to general base-catalysis, which in the active site of RNR was proposed to be assured by E441.[23] Other examples include the successful reproduction of the cascade reaction occurring at the active site upon activation of the substrate.[49,24,25] The first unambiguous proof regarding the viability of the abstraction of the 3′-H by a thiyl group was then obtained. Applied to inhibition studies, such reactions clearly demonstrate that, upon selective generation of 3′ radicals in N*cl*DP and N*z*DP analogues in refluxing toluene (see above), the analogues eliminated radical chlorine, and not anionic chloride, thus giving support to a new fundamental mechanistic alternative for the reaction.[46–49] However, one of the first conclusions of this study was that both 2′ substituents (chloride and azide) were eliminated as anions. Such contradiction needs to be explained if the present results are to be considered as definitive. Based on our previous knowledge about the chemistry of this enzyme, and by looking at the two systems (the enzymatic and the biomimetic), we noted an important difference: the biomimetic systems do not include a basic group capable of protonating/deprotonating the 3′-HO group. Such function is crucial for the enzyme, since it allows the transfer of charge from and into the substrate as needed. That functionality in the enzyme is assured by E441, which was demonstrated to be fundamental to several enzymatic reaction steps.[29] Applied to the activation of the inhibitors we can easily see that the basic function is crucial for this reaction. Hence, with the basic function present, the inhibitor can eliminate an anion without generating a system with a charge separation. An anion is eliminated from the 2′ position and a cation (proton) is eliminated from the 3′-HO group, thus avoiding the charge separation. However, without E441 (as happens in the biomimetic experiments using the inhibitor analogues) the elimination of an anion will result in a system with a charge separation: a negative charge in the leaving substituent and a positive charge—an unstable carbocation radical—in the 2′-C position (Scheme 2). This seems to be the reason why in biomimetic experiments the substituents are not eliminated as anions.

To verify our hypothesis, we performed theoretical calculations on simple model systems. We used two different systems, both including inhibitor model **1**. One of the systems included the E441 residue (system A; Scheme 2) and the

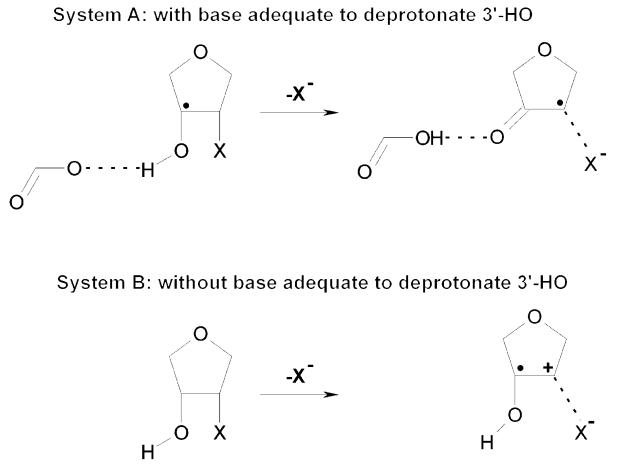

Scheme 2. Elimination of the 2′-substituents as anions with (top) and without (bottom) a basic group able to deprotonate 3′-HO.

other system did not (system B). We started by optimizing the geometry of both systems, and afterwards simply deleted the 3′-H atom and re-optimized the geometry. System A spontaneously transferred the proton from the 3′-HO group to E441 and eliminated anionic chloride. However, as predicted, system B did not eliminate the substituent spontaneously. By scanning along the 2′-C–Cl bond we verified that system B has to cross a barrier of about 20 kcal mol^{-1} to be able to eliminate the substituent, which indeed leaves as a radical. As biomimetic experiments were performed in benzene/toluene, which is known to stabilize chlorine radicals,[37, 49] it seems evident that elimination of the substituent as radical chlorine will occur also in the organic solvent, and (probably) with a lower barrier than in the gas phase. This reasoning makes it unnecessary to consider the presence of the solvent in these particular calculations.

Thus we concluded that the nature of the leaving substituent can be controlled; it will be anionic or radical depending on the presence or absence of a basic residue capable of deprotonating the 3′-HO group. In the enzyme such functionality does exist, and so it can be concluded that the enzyme indeed eliminates anions, and not radicals. We suggest that biomimetic experiments with inhibitor analogues can be made even more reliable if such functionality is included, as was done previously by Giese and co-workers for the natural substrate.[23]

Conclusion

This work was devoted to the study of the inhibition of RNR by 2′-substituted nucleotide analogues. The main objectives were to understand what determines which enzyme dimer will be inhibited by which inhibitor, and to investigate an alternative mechanistic proposal, which considered the 2′ substituents as being eliminated as radicals (not anions), thus leading to further reactions between the substituent and the redox-active cysteines, not present in the actual model. The obtained results allowed us to clarify all these points. Our first conclusion was that the initial abstraction of the 3′-H atom by the radical C439 was coupled with a proton transfer from the 3′-HO group to E441 and with the elimination of the substituent. Such spontaneous decomposi-

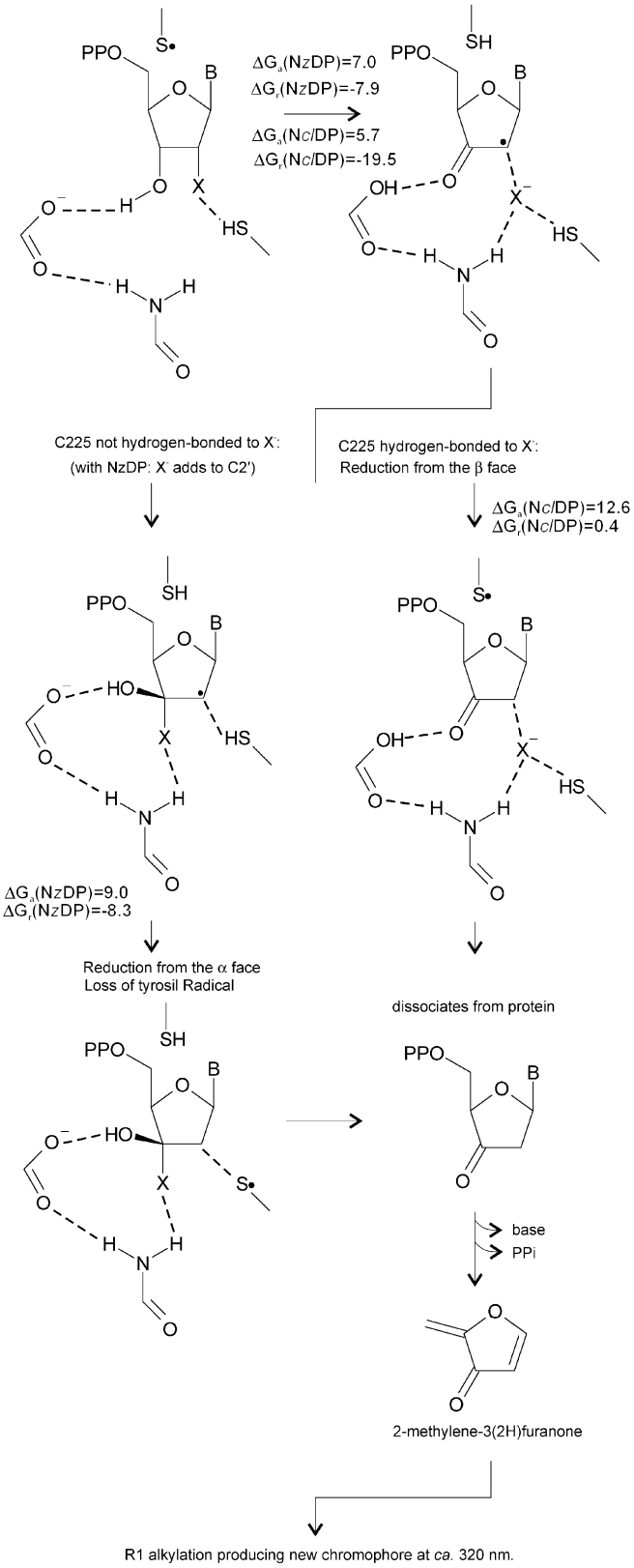

Scheme 3. A refined rational version of the model for RNR inhibition by 2′-substituted substrate analogues, taking into consideration the results obtained herein. Relevant energies are depicted in kcal mol^{-1}.

tion of the inhibitors was unknown, and contrasts with the behavior of the natural substrate, which does not decompose similarly. It was believed beforehand that such transformations would occur in a stepwise fashion, through (at least) two elementary steps (as in Scheme 1). After the decomposition of the inhibitor two major pathways are possible, reduction from the α face (leading to R2 inhibition) or from the β face (leading to R1 inhibition without affecting R2). Our results allow us to conclude that reduction from the α face will occur if the substituent does not hinder the approach of C225 to the 2′-C atom, through the formation of hydrogen bonds. This was the case for N*z*DP, which adds to the 3′-C atom before reduction of the 2′-C radical. If the substituent becomes hydrogen-bonded to C225, and thereby hinders the access of C225 to the 2′-C radical, reduction occurs from the β face, through C439. In that case the radical is regenerated at R2 and inhibition results from alkylation of R1. Taking these conclusions into account we updated the model for inhibition (Scheme 3).

Another important conclusion of this work is that substituents are eliminated as anions in the enzymatic reaction, and not as radicals. Model calculations clarified that the nature of the leaving substituent (radical/anionic) depends on the presence of a base capable of deprotonating the 3′-HO group. If such a base is present (as in the case of RNR) the substituents are eliminated as anions. However, if the base is omitted (as in biomimetic experiments using inhibitor analogues) the substituents are eliminated as anions. This should provide a general way to control the nature of the eliminated 2′ substituents from substituted ribonucleotides.

Acknowledgement

Fundação para a Ciência e Tecnologia (Project POCTI/35736/99, Portugal) and the National Foundation for Cancer Research (NFCR-USA) are gratefully acknowledged for financial support.

[1] J. Stubbe, W. A. van der Donk, *Chem. Rev.* **1998**, *98*, 705.
[2] S. Eriksson, B.-M. Sjöberg in *Allosteric Enzymes*, (Ed.: G. Hervé), CRC, Boca Raton, **1989**, p. 189.
[3] J. Stubbe, *Adv. Enzymol. Relat. Areas Mol. Biol.* **1990**, *63*, 349.
[4] P. Reichard, *Science* **1993**, *260*, 1773.
[5] J. Stubbe, W. A. van der Donk, *Chem. Biol.* **1995**, *2*, 793.
[6] B.-M. Sjöberg in *Nucleic Acids and Molecular Biology, Vol. 9*, (Eds.: F. Eckstein, D. Lilley), Springer, Berlin, **1995**, pp. 192.
[7] J. G. Cory, P. Chiba, in *Combination Chemotherapy Directed at the Components of Nucleoside Diphosphate Reductase*, (Eds.: J. G. Cory, A. H. Cory), Pergamon Press, New York, **1989**, p. 245.
[8] M. J. Robins, M. C. Samano, V. Samano, *Nucleosides Nucleotides* **1995**, *14*, 485.
[9] J. Nocentini, *Crit. Rev. Oncol. Hematol.* **1996**, *22*, 89.
[10] G. J. Gerfen, W. A. van der Donk, G. Yu, J. R. McCarthy, E. T. Jarvi, D. P. Matthews, C. Farrar, R. G. Griffin, J. Stubbe, *J. Am. Chem. Soc.* **1998**, *120*, 3823.
[11] J. R. McCarthy, P. S. Sunkara, *Design, Synthesis and Anti-tumor Activity of an Inhibitor of Ribonucleotide Reductase* (Eds.: D. B. Weiner, W. B. Williams), CRC Press, Boca Raton, FL, **1995**, pp. 3–32.
[12] J. R. McCarthy, P. S. Sunkara, D. P. Matthews, A. J. Bitonti, E. T. Jarvi, J. S. Sabol, R. J. Resvick, E. W. Hubber, W. A. van der Donk, G. Yu, J. Stubbe, *ACS Symp. Ser.* **1996**, *639*, 246.
[13] A. J. Bitonti, J. A. Dumont, T. L. Bush, E. A. Cashman, D. E. Crossdoersen, P. S. Wright, D. P. Matthews, J. R. McCarthy, D. A. Kaplan, *Cancer Res.* **1994**, *54*, 1485.
[14] A. J. Bitonti, T. L. Bush, M. T. Lewis, P. S. Sunkara, *Anticancer Res.* **1995**, *15*, 1179.
[15] R. P. Abratt, *Anti-Cancer Drugs* **1995**, *6*, 63.
[16] L. W. Hertel, J. S. Kroin, C. S. Grossman, G. B. Grindey, A. F. Dorr, A. M. V. Storniolo, W. Plunkett V. Gandhi, P. Huang, *ACS Symp. Ser.* **1996**, *639*, 265
[17] E. Hammersten, P. Reichard, E. Saluste, *J. Biol. Chem.* **1950**, *183*, 105.
[18] P. Reichard, B. Estborn, *J. Biol. Chem.* **1951**, *188*, 839.
[19] R. L. Blackley, H. A. Barker, *Biochem. Biophys. Res. Commun.* **1964**, *16*, 391.
[20] H. S. Beck, J. Hardy, *Proc. Natl. Acad. Sci. USA* **1965**, *54*, 286.
[21] T. Barlow, *Biochem. Biophys. Res. Commun.* **1988**, *155*, 747.
[22] M. Fontecave, R. Eliasson, P. Reichard, *Proc. Natl. Acad. Sci. USA* **1989**, *86*, 2147.
[23] R. Lenz, and B. Giese, *J. Am. Chem. Soc.* **1997**, *119*, 2784.
[24] M. Robins, G. Ewing, *J. Am. Chem. Soc.* **1999**, *121*, 5823.
[25] Z. Guo, M. Samano, J. Krzykawski, S. Wnuk, G. Ewing, M. Robins, *Tetrahedron* **1999**, *55*, 5705.
[26] P. E. M. Siegbahn, L. Eriksson, F. Himo, M. J. Pavlov, *J. Phys. Chem. B* **1998**, *102*, 10622.
[27] M. Eriksson, U. Uhlin, S. Ramaswamy, M. Ekberg, K. Regnstrom, B.-M. Sjöberg, H. Eklund, *Structure (London)* **1997**, *5*, 1077.
[28] J. Stubbe, J. Ge, C. Yee, *Trends Biochem. Sci.* **2001**, *26*, 93.
[29] A. Kasrayan, A. Persson, M. Sahlin, B.-M. Sjöberg, *J. Biol. Chem.* **2002**, *277*, 5749.
[30] L. Thelander, B. Larsson, *J. Biol. Chem.* **1976**, *251*, 1398.
[31] J. Stubbe, J. Kozarich, *J. Biol. Chem.* **1980**, *255*, 5511.
[32] J. Stubbe, J. Kozarich, *J. Am. Chem. Soc.* **1980**, *102*, 2505.
[33] B.-M. Sjöberg, A. Gräslund, F. Eckstein, *J. Biol. Chem.* **1983**, *258*, 8060.
[34] M. Ator, S. Salowe, J. Stubbe, M. Emptage, M. Robins, *J. Am. Chem. Soc.* **1984**, *106*, 1886.
[35] G. Harris, M. Ator, J. Stubbe, *Biochemistry* **1984**, *23*, 5214.
[36] M. Ator, J. Stubbe, *Biochemistry* **1985**, *24*, 7214.
[37] Susana Pereira, Pedro Alexandrino Fernandes, Maria João Ramos, unpublished results.
[38] S. Salowe, M. Ator, J. Stubbe, *Biochemistry* **1987**, *26*, 3408.
[39] J. Stubbe, *Adv. Enzymol.***1989**, *63*, 349.
[40] C. Baker, J. Banzon, J. Bollinger, J. Stubbe, V. Samano, J. Robins, B. Lippert, R. Jarvi, R. Resvick, *J. Med. Chem.* **1991**, *34*, 1879.
[41] V. Samano, J. Robins, *J. Org. Chem.* **1991**, *56*, 7108.
[42] J. Robins, V. Samano, W. Zhang, J. Balzarini, E. De Clercq, R. Borchardt, Y. Lee, C.-S. Yuan, *J. Med. Chem.* **1992**, *35*, 2283.
[43] W. van der Donk, J. Stubbe, G. Gerfen, B. Bellew, R. Griffin, *J. Am. Chem. Soc.* **1995**, *117*, 8908
[44] S. Auguste, D. Young, *J. Chem. Soc. Perkin Trans.* **1995**, 395.
[45] W. van der Donk, G. Yu, D. Silva, J. Stubbe, J. McCarthy, E. Jarvi, D. Matthews, R. Resvick, E. Wagner, *Biochemistry* **1996**, *35*, 8381..
[46] M. Robins, S. Wnuk, A. Hernández-Thirring, M. Samano, *J. Am. Chem. Soc.* **1996**, *118*, 11341.
[47] M. Robins, Z. Guo, M. Samano, S. Wnuk, *J. Am. Chem. Soc.* **1996**, *118*, 11317.
[48] M. Robins, Z. Guo, S. Wnuk, *J. Am. Chem. Soc.* **1997**, *119*, 3637.
[49] M. Robins, Z. Guo, M. Samano, S. Wnuk, *J. Am. Chem. Soc.* **1999**, *121*, 1425.
[50] L. de Fallois, J.-L. Décout, M. Fontecave, *J. Chem. Soc. Perkin Trans. 1* **1997**, 2587.
[51] W. van der Donk, G. Gerfen, J. Stubbe, *J. Am. Chem. Soc.* **1998**, *120*, 4252.
[52] W. van der Donk, G. Yu, L. Pérez, R. Sanchez, J. Stubbe, V. Samano, M. Robins, *Biochemistry* **1998**, *37*, 6419.
[53] L. Eriksson, *J. Am. Chem. Soc.* **1998**, *120*, 8051.
[54] S. Salowe, J. Bollinger, M. Ator, J. Stubbe, J. McCracken, J. Peisash, *Biochemistry* **1993**, *32*, 12749.
[55] S. Manfredini, P. Baraldi, E. Durini, S. Vertuani, J. Balzarini, E. De - Clerck, A. Karlsson, V. Buzzoni, L. Thelanders, *J. Med. Chem.* **1999**, *42*, 3243.
[56] G. A. Russell, *J. Am. Chem. Soc.* **1958**, *80*, 4987.

[57] Gaussian 98, Revision A.9, M. J. Frisch, G. W. Trucks, H. B. Schlegel, G. E. Scuseria, M. A. Robb, J. R. Cheeseman, V. G. Zakrzewski, J. A. Montgomery, Jr., R. E. Stratmann, J. C. Burant, S. Dapprich, J. M. Millam, A. D. Daniels, K. N. Kudin, M. C. Strain, O. Farkas, J. Tomasi, V. Barone, M. Cossi, R. Cammi, B. Mennucci, C. Pomelli, C. Adamo, S. Clifford, J. Ochterski, G. A. Petersson, P. Y. Ayala, Q. Cui, K. Morokuma, D. K. Malick, A. D. Rabuck, K. Raghavachari, J. B. Foresman, J. Cioslowski, J. V. Ortiz, A. G. Baboul, B. B. Stefanov, G. Liu, A. Liashenko, P. Piskorz, I. Komaromi, R. Gomperts, R. L. Martin, D. J. Fox, T. Keith, M. A. Al-Laham, C. Y. Peng, A. Nanayakkara, M. Challacombe, P. M. W. Gill, B. Johnson, W. Chen, M. W. Wong, J. L. Andres, C. Gonzalez, M. Head-Gordon, E. S. Replogle, J. A. Pople, Gaussian, Inc. Pittsburgh PA, **1998**.
[58] A. D. Becke, *J. Chem. Phys.* **1993**, *98*, 5648.
[59] C. Lee, W. Yang, R. J. Parr, *Phys. Rev. Sect. B* **1998**, *37*, 785.
[60] R. W. Hertwig, W. Koch, *J. Comput. Chem.* **1995**, *16*, 576.
[61] P. Siegbahn, *J. Am. Chem. Soc.* **1998**, *120*, 8417.
[62] J. Forrester, Æ. Frisch, in *Exploring Chemistry with Electronic Structure Methods*, Gaussian Inc., Pittsburgh, **1996**, pp. 64 and 157.
[63] P. A. Fernandes, L. A. Eriksson, M. J. Ramos, *Theor. Chem. Acc.* **2002**, *108*, 352.
[64] M. R. A. Blomberg, P. E. M. Siegbahn, G. T. Babcock, *J. Am. Chem. Soc.* **1998**, *120*, 8812.
[65] R. S. Mulliken, *J. Chem. Phys.* **1955**, *23*, 1833.
[66] F. Himo, L. A. Eriksson, Catalytic Reactions of Radical Enzymes in *Theoretical Biochemistry–Processes and Properties of Biological Systems* (Ed.: L. A. Eriksson), Elsevier, **2001.**
[67] J. Stubbe, M. Ator, T. Krenitsky, *J. Biol. Chem.* **1983**, *258*, 1625.

Received: March 14, 2003 [F4948]

